

Unbiased Hamiltonian Monte Carlo with couplings

Jeremy Heng* and Pierre E. Jacob*

March 28, 2025

Abstract

We propose a coupling approach to parallelize Hamiltonian Monte Carlo estimators, following Jacob, O’Leary & Atchadé (2017). A simple coupling, obtained by using common initial velocities and common uniform variables for the acceptance steps, leads to pairs of Markov chains that contract, in the sense that the distance between them can become arbitrarily small. We show how this strategy can be combined with coupled random walk Metropolis–Hastings steps to enable exact meetings of the two chains, and in turn, unbiased estimators that can be computed in parallel and averaged. The resulting estimator is valid in the limit of the number of independent replicates, instead of the usual limit of the number of Markov chain iterations. We investigate the effect of tuning parameters, such as the number of leap-frog steps and the step size, on the estimator’s efficiency. The proposed methodology is demonstrated on a 250-dimensional Normal distribution, on a bivariate Normal truncated by linear and quadratic inequalities, and on a logistic regression with 300 covariates.

1 Introduction

1.1 Goal: parallel computation with Hamiltonian Monte Carlo

Hamiltonian Monte Carlo, also called Hybrid Monte Carlo (HMC), is a Markov chain Monte Carlo (MCMC) method to approximate integrals with respect to a target probability distribution π on \mathbb{R}^d . Originally proposed by Duane et al. [1987] in the physics literature, it was later introduced in statistics by Neal [1993] and is now part of the standard toolbox [Brooks et al., 2011, Lelièvre et al., 2010], in part due to favorable scaling properties with respect to the dimension d [Beskos et al., 2010, 2013], compared to e.g. random walk Metropolis–Hastings. Hamiltonian Monte Carlo is at the core of the No-U-Turn sampler (NUTS, Hoffman and Gelman [2014]) used in the software Stan [Carpenter et al., 2016]. As with any other MCMC method, HMC estimators are justified in the limit of the number of iterations. Algorithms which rely on such asymptotics face the risk of becoming obsolete if computational power keeps increasing through the number of available processors and not through clock speed. To address this issue, we propose to run pairs of HMC chains, for a random but finite number of iterations, and combine them in such a way that the resulting estimators are unbiased. One can then produce independent copies in parallel and average them to obtain estimators that are valid in the limit of the number of copies.

If the chains could be initialized from the target distribution, MCMC estimators would be unbiased, and one could simply average independent chains [Rosenthal, 2000]. Perfect samplers can be used for this purpose [Casella et al., 2001, Huber, 2016, Glynn, 2016]; more widely applicable approaches to unbiased estimation from MCMC samplers are proposed in e.g. Mykland et al. [1995], Neal [2002]. More recently, Jacob et al. [2017b] present an approach based on coupled Markov chains. The method builds upon Glynn and Rhee [2014], Jacob et al. [2017a] and other “debiasing” techniques [Jacob and Thiery, 2015, Vihola, 2015, Glynn, 2016], and leverages maximal couplings [Thorisson, 2000] of proposal and conditional distributions to remove the “burn-in bias” of Metropolis–Hastings and Gibbs chains respectively. The use of maximal couplings allows two chains initialized at different positions to coincide exactly after a random number of steps, referred to as the meeting time. Importantly, these constructions are applicable to continuous state spaces.

The present article proposes a combination of couplings to enable parallel computation for the Hamiltonian Monte Carlo sampler. We start by briefly recalling the unbiased estimators of Jacob et al. [2017b] in Section 1.2 and introducing some preliminary notation in Section 1.3. The R code producing the figures of this article is available on the GitHub account of the second author¹.

*Department of Statistics, Harvard University, USA. Emails: jjmheng@fas.harvard.edu & pjacob@fas.harvard.edu.

¹Link: github.com/pierrejacob/debiasedhmc.

1.2 Context: unbiased estimation with couplings

Consider the task of approximating the integral $\pi(h) = \int h(x)\pi(dx) < \infty$, for a test function h of interest. Let $X = (X_n)_{n \geq 0}$ denote a π -invariant MCMC chain associated with an initial distribution π_0 and transition kernel P , i.e. $X_0 \sim \pi_0$ and $X_n \sim P(X_{n-1}, \cdot)$ for all $n \geq 1$. Introduce another Markov chain $Y = (Y_n)_{n \geq 0}$ which has the same law as $X = (X_n)_{n \geq 0}$, so that X_n and Y_n have the same marginal distribution for all $n \geq 0$. We will write \mathbb{P} to denote the law of the coupled chain $(X_n, Y_n)_{n \geq 0}$ and \mathbb{E} to denote expectation with respect to \mathbb{P} . We now assume the following.

- [A1] As $n \rightarrow \infty$, $\mathbb{E}[h(X_n)] \rightarrow \pi(h)$, and there exists $\iota > 0$ and $D < \infty$ such that for all $n \geq 0$, $\mathbb{E}[h(X_n)^{2+\iota}] < D$.
- [A2] The meeting time $\tau = \inf \{n \geq 1 : X_n = Y_{n-1}\}$ is finite almost surely, and satisfies a geometric tail condition of the form $\mathbb{P}(\tau > n) \leq C\gamma^n$ for all $n \geq 0$ and some constants $C < \infty$ and $\gamma \in (0, 1)$.
- [A3] The coupled chains are faithful [Rosenthal, 1997]: $X_n = Y_{n-1}$ for all $n \geq \tau$.

Under these assumptions, the random variable defined as

$$H_k(X, Y) = h(X_k) + \sum_{n=k}^{\max(k, \tau-1)} \{h(X_{n+1}) - h(Y_n)\}, \quad (1)$$

is an unbiased estimator of $\pi(h)$, for any choice of initial distribution π_0 and any $k \geq 0$. The first term above, $h(X_k)$, is in general biased since the chain $(X_n)_{n \geq 0}$ might not have reached stationarity by step k . As the second term is precisely such that $\mathbb{E}[H_k(X, Y)] = \pi(h)$, it is referred to as a correction term. If $k \geq \tau$, the correction term is zero. The estimator can be computed in $\max(\tau, k)$ steps, which has a finite expectation under **A2**.

We introduce another unbiased estimator, denoted by $\bar{H}_{k:m}$, defined for some integer $m > k$, resulting from averaging $H_\ell(X, Y)$ over $\ell \in \{k, \dots, m\}$. By rearranging terms, we define

$$\bar{H}_{k:m}(X, Y) = \frac{1}{m-k+1} \sum_{n=k}^m h(X_n) + \frac{1}{m-k+1} \sum_{n=k}^{\max(m, \tau-1)} \min(n-k+1, m-k+1) \{h(X_{n+1}) - h(Y_n)\}, \quad (2)$$

which is unbiased and computable in $\max(\tau, m)$ steps. The first average above can be recognized as the usual MCMC estimator, obtained after m iterations and discarding the first $k-1$ states. As before, the second term can be seen as a correction to remove the bias of $\bar{H}_{k:m}(X, Y)$. On the event $\{k \geq \tau\}$, the correction term is equal to zero. We refer to Jacob et al. [2017b] for a more detailed discussion of (1)-(2), and guidelines for the choice of k and m . Importantly, unbiased estimators can be produced independently in parallel and averaged, with direct computational gains on parallel computing architectures. Explicit constructions of pairs of Markov chains satisfying **A1-A3** based on Metropolis–Hastings and Gibbs samplers are given in Jacob et al. [2017b]. Here we propose coupling strategies for HMC chains, so as to enable the unbiased estimators of (1)-(2). The main challenge lies in **A2**, for which two coupled chains have to meet exactly after a “Geometric” number of steps.

1.3 Notation and plan

The set of integers $\{a, \dots, b\}$ for $a \leq b$ is written as $[a : b]$. The set of non-negative real numbers is denoted by \mathbb{R}_+ . The vectors 0_d and 1_d refer to d -dimensional vectors of zeros and ones respectively. The matrix I_d is the identity matrix of size $d \times d$. The norm of a vector $x \in \mathbb{R}^d$ is written as $|x| = (\sum_{i=1}^d x_i^2)^{1/2}$. The transpose of a vector $x \in \mathbb{R}^d$ and matrix $A \in \mathbb{R}^{d \times p}$ are denoted by x^T and A^T respectively. The gradient of a function $(x, y) \mapsto f(x, y)$ with respect to x (resp. y) is denoted by $\nabla_x f$ (resp. $\nabla_y f$). The Hessian of a real-valued function f is denoted by $\nabla^2 f$. The Borel σ -algebra of \mathbb{R}^d is denoted by $\mathcal{B}(\mathbb{R}^d)$ and the Lebesgue measure on \mathbb{R}^d by Leb_d . The Normal distribution with mean μ and covariance matrix Σ is denoted by $\mathcal{N}(\mu, \Sigma)$ and its density by $x \mapsto \mathcal{N}(x; \mu, \Sigma)$. The Uniform distribution on the interval $[0, 1]$ is $\mathcal{U}[0, 1]$. The total variation distance d_{TV} between two distributions, with densities p and q , is defined as $d_{\text{TV}}(p, q) = 1/2 \int |p(x) - q(x)|dx$.

The rest of the article is structured as follows. Section 2 describes Hamiltonian dynamics for coupled trajectories. Section 3 introduces a simple coupling of Hamiltonian Monte Carlo chains, which satisfies a relaxed meeting time assumption similar to **A2**. Section 4 then combines HMC kernels with random walk Metropolis–Hastings kernels, to ensure that chains meet exactly and satisfy **A2**. Section 5 contains simulation results on a 250-dimensional Normal target, a truncated Normal distribution and a logistic regression with 300 covariates, and Section 6 concludes.

2 Hamiltonian dynamics for pairs of particles

2.1 Hamiltonian flows and extended target

We now suppose that the target distribution has the form

$$\pi(dq) \propto \exp(-U(q))dq,$$

where the potential $U : \mathbb{R}^d \rightarrow \mathbb{R}_+$ is twice continuously differentiable and its gradient ∇U is globally β -Lipschitz, i.e. there exists $\beta > 0$ such that

$$|\nabla U(q) - \nabla U(q')| \leq \beta|q - q'|,$$

for all $q, q' \in \mathbb{R}^d$. We now introduce Hamiltonian flows on a phase space \mathbb{R}^{2d} , which consists of position variables $q \in \mathbb{R}^d$ and velocity variables $p \in \mathbb{R}^d$. We will be concerned with a Hamiltonian function $E : \mathbb{R}^d \times \mathbb{R}^d \rightarrow \mathbb{R}_+$ of the form

$$E(q, p) = U(q) + \frac{1}{2}|p|^2.$$

We note the use of an identity mass matrix here and defer to preconditioning as a means to incorporate any knowledge of the curvature properties of π . The time evolution of a particle $(q(t), p(t))_{t \in \mathbb{R}_+}$ under Hamiltonian dynamics is described by the autonomous system of ordinary differential equations

$$\begin{aligned} \frac{d}{dt}q(t) &= \nabla_p E(q(t), p(t)) = p(t), \\ \frac{d}{dt}p(t) &= \nabla_q E(q(t), p(t)) = -\nabla U(q(t)). \end{aligned} \tag{3}$$

Under the above assumptions on U , (3) with an initial condition $(q(0), p(0)) = (q_0, p_0) \in \mathbb{R}^d \times \mathbb{R}^d$ admits a unique solution globally on \mathbb{R}_+ [Lelièvre et al., 2010, p. 14]. We will write the flow map as $\Phi_t(q_0, p_0) = (q(t), p(t))$ for any $t \in \mathbb{R}_+$, and $\Phi_t^\circ(q_0, p_0) = q(t)$ and $\Phi_t^*(q_0, p_0) = p(t)$ as its projection onto the position and velocity coordinates respectively. It is worth recalling that Hamiltonian flows have the following properties.

- [P1] (Reversibility) $\Phi_t^{-1} = M \circ \Phi_t \circ M$ where $M(q, p) := (q, -p)$ denotes velocity reversal;
- [P2] (Energy conservation) $E \circ \Phi_t = E$ for any $t \in \mathbb{R}_+$;
- [P3] (Volume preservation) $\text{Leb}_{2d}(\Phi_t(A)) = \text{Leb}_{2d}(A)$ for any $A \in \mathcal{B}(\mathbb{R}^d \times \mathbb{R}^d)$.

It follows from **P1** and **P2** that the extended target distribution on phase space,

$$\tilde{\pi}(dq, dp) \propto \exp(-E(q, p))dqdp,$$

is invariant under the Markov semi-group induced by the flow, i.e. the pushforward measure $\Phi_t \sharp \tilde{\pi}$ defined by $\Phi_t \sharp \tilde{\pi}(A) = \tilde{\pi}(\Phi_t^{-1}(A))$ for $A \in \mathcal{B}(\mathbb{R}^{2d})$ is equal to $\tilde{\pi}$ for any $t \in \mathbb{R}_+$.

2.2 Coupled Hamiltonian dynamics

Following Section 1.2, we now consider the coupling of two particles $(q^i(t), p^i(t))_{t \in \mathbb{R}_+}$, $i = 1, 2$ evolving under (3) with initial conditions $(q^i(0), p^i(0)) = (q_0^i, p_0^i)$, $i = 1, 2$. We first draw some insights from a Gaussian example.

Example 1. Let π be a Gaussian distribution on \mathbb{R} with mean $\mu \in \mathbb{R}$ and unit variance $\sigma^2 \in \mathbb{R}_+$, in which case $U(q) = (q - \mu)^2/(2\sigma^2)$ and $\nabla U(q) = (q - \mu)/\sigma^2$. Then the solution of (3) is given by

$$\Phi_t(q_0, p_0) = \begin{pmatrix} \mu + (q_0 - \mu) \cos\left(\frac{t}{\sigma}\right) + \sigma p_0 \sin\left(\frac{t}{\sigma}\right) \\ p_0 \cos\left(\frac{t}{\sigma}\right) - \frac{1}{\sigma}(q_0 - \mu) \sin\left(\frac{t}{\sigma}\right) \end{pmatrix},$$

see e.g. Neal [2011]. Hence the difference between the positions is given by

$$q^1(t) - q^2(t) = (q_0^1 - q_0^2) \cos\left(\frac{t}{\sigma}\right) + \sigma(p_0^1 - p_0^2) \sin\left(\frac{t}{\sigma}\right).$$

Observe that if we set $p_0^1 = p_0^2$, then

$$|q^1(t) - q^2(t)| = |q_0^1 - q_0^2| \cos\left(\frac{t}{\sigma}\right),$$

so the particles meet exactly whenever $t = (2a + 1)\pi\sigma/2$, and contraction occurs for any $t \neq \pi a \sigma$, for any non-negative integer a .

This example motivates a coupling that simply assigns particles the same initial velocity. Moreover, it also reveals that certain trajectory lengths will result in stronger contractions than others. We now examine the utility of this approach more generally. Define $\Delta(t) = q^1(t) - q^2(t)$ as the difference between the particle locations and note that

$$\frac{1}{2} \frac{d}{dt} |\Delta(t)|^2 = \Delta(t)^T (p^1(t) - p^2(t)).$$

Therefore by imposing that $p^1(0) = p^2(0)$, the function $t \mapsto |\Delta(t)|$ admits a stationary point at time $t = 0$. This is geometrically intuitive as the trajectories at time zero are parallel to one another for an infinitesimally small amount of time. To characterize this stationary point, we compute

$$\frac{1}{2} \frac{d^2}{dt^2} |\Delta(t)|^2 = -\Delta(t)^T (\nabla U(q^1(t)) - \nabla U(q^2(t))) + |p^1(t) - p^2(t)|^2.$$

If we assume that the potential U is α -strongly convex in an open set $S \in \mathcal{B}(\mathbb{R}^d)$, i.e. there exists $\alpha > 0$ such that

$$(\nabla U(q) - \nabla U(q'))^T (q - q') \geq \alpha |q - q'|^2,$$

for all $q, q' \in S$, then

$$\frac{1}{2} \frac{d^2}{dt^2} |\Delta(t)|^2 \leq -\alpha |q^1(t) - q^2(t)|^2 + |p^1(t) - p^2(t)|^2. \quad (4)$$

Therefore by the second derivative test, $t = 0$ is a strict local maximum point if $q_0^1, q_0^2 \in S$. Using continuity of $t \mapsto |\Delta(t)|^2$, it follows that there exist $\tilde{t} > 0$ and $\rho < 1$ such that

$$|\Phi_t^\circ(q_0^1, p_0) - \Phi_t^\circ(q_0^2, p_0)| < \rho |q_0^1 - q_0^2|,$$

for $t \in (0, \tilde{t})$. We note the dependence of \tilde{t} and ρ on the initial positions (q_0^1, q_0^2) and velocity p_0 . We now strengthen the above claim.

Lemma 1. *Suppose that the potential U is twice continuously differentiable, α -strongly convex on $S \in \mathcal{B}(\mathbb{R}^d)$ and its gradient ∇U is globally β -Lipschitz. For any compact set $C \subset S \times S \times \mathbb{R}^d$, there exist $\tilde{t} > 0$ and $\rho < 1$ such that*

$$|\Phi_t^\circ(q_0^1, p_0) - \Phi_t^\circ(q_0^2, p_0)| \leq \rho |q_0^1 - q_0^2|, \quad (5)$$

for all $(q_0^1, q_0^2, p_0) \in C$ and $t \in (0, \tilde{t})$.

Proof. Take $(q_0^1, q_0^2, p_0) \in C$. Applying Taylor's theorem on $\Delta(t)$ around $t = 0$ gives

$$\Delta(t) = \Delta(0) - \frac{1}{2} t^2 G_0 - \frac{1}{6} t^3 G_*,$$

for some $t^* \in (0, t)$, where $G_0 := \nabla U(q_0^1) - \nabla U(q_0^2)$ and $G_* := \nabla^2 U(q^1(t^*)) p^1(t^*) - \nabla^2 U(q^2(t^*)) p^2(t^*)$. We will control each term of the expansion

$$|\Delta(t)|^2 = |\Delta(0)|^2 - t^2 \Delta(0)^T G_0 - \frac{1}{3} t^3 \Delta(0)^T G_* + \frac{1}{4} t^4 |G_0|^2 + \frac{1}{6} t^5 G_0^T G_* + \frac{1}{36} t^6 |G_*|^2.$$

Using strong convexity, the Lipschitz assumption and Young's inequality

$$|\Delta(t)|^2 \leq \left(1 - \alpha t^2 + \frac{1}{6} t^3 + \frac{1}{4} \beta^2 t^4 + \frac{1}{12} \beta^2 t^5\right) |\Delta(0)|^2 + \left(\frac{1}{6} t^3 + \frac{1}{12} t^5 + \frac{1}{36} t^6\right) |G_*|^2.$$

Note that by Young's inequality and the Lipschitz assumption

$$\begin{aligned} |G_*|^2 &\leq 2 \|\nabla^2 U(q^1(t^*))\|_2^2 |p^1(t^*)|^2 + 2 \|\nabla^2 U(q^2(t^*))\|_2^2 |p^2(t^*)|^2 \\ &\leq 2\beta^2 (|\Phi_{t^*}^*(q_0^1, p_0)|^2 + |\Phi_{t^*}^*(q_0^2, p_0)|^2) \\ &\leq 2\beta^2 \sup_{(q_0^1, q_0^2, p_0) \in C} (|\Phi_{t^*}^*(q_0^1, p_0)|^2 + |\Phi_{t^*}^*(q_0^2, p_0)|^2), \end{aligned}$$

where $\|\cdot\|_2$ denotes the spectral norm. The above supremum is attained by continuity of the mapping $(q, p) \mapsto \Phi_{t^*}^*(q, p)$. The claim (5) follows by combining both inequalities and taking t sufficiently small. \square

3 Hamiltonian Monte Carlo

3.1 Leap frog integrator

As the flow defined by (3) is typically intractable, one has to resort to time discretization. The leap-frog symplectic integrator is a standard choice as it preserves **P1** and **P3**. Given a step size $\varepsilon > 0$ and a number of leap-frog steps $L \in \mathbb{N}$, this scheme initializes at $(q_0, p_0) \in \mathbb{R}^d \times \mathbb{R}^d$ and iterates

$$\begin{aligned} p_{\ell+1/2} &= p_\ell - \frac{\varepsilon}{2} \nabla U(q_\ell) \\ q_{\ell+1} &= q_\ell + \varepsilon p_{\ell+1/2} \\ p_{\ell+1} &= p_{\ell+1/2} - \frac{\varepsilon}{2} \nabla U(q_{\ell+1}), \end{aligned}$$

for $\ell \in [0 : L-1]$. We write the leap-frog iteration as $\hat{\Phi}_\varepsilon(q_\ell, p_\ell) = (q_{\ell+1}, p_{\ell+1})$ and the corresponding approximation of the flow as $\hat{\Phi}_{\varepsilon, \ell}(q_0, p_0) = (q_\ell, p_\ell)$ for $\ell \in [1 : L]$. As before, we denote by $\hat{\Phi}_{\varepsilon, \ell}^\circ(q_0, p_0) = q_\ell$ and $\hat{\Phi}_{\varepsilon, \ell}^*(q_0, p_0) = p_\ell$ the projections onto the position and velocity coordinates respectively. The leap-frog scheme is of order two [Hairer et al., 2005, Theorem 3.4]: for sufficiently small ε , we have both

$$|\hat{\Phi}_{\varepsilon, L}(q_0, p_0) - \Phi_{\varepsilon L}(q_0, p_0)| \leq C_1 \varepsilon^2, \quad (6)$$

and

$$|E(\hat{\Phi}_{\varepsilon, L}(q_0, p_0)) - E(q_0, p_0)| \leq C_2 \varepsilon^2, \quad (7)$$

for some constants $C_1, C_2 > 0$. Given the nature of Hamiltonian dynamics, the constant C_1 will typically grow exponentially with the number of leap-frog iterations L [Leimkuhler and Matthews, 2015, Section 2.2.3]. Under appropriate assumptions, the constant C_2 on the other hand can be shown to be stable over exponentially long time intervals [Hairer et al., 2005, Theorem 8.1]. The Hamiltonian is not exactly conserved under time discretization, but one can employ a Metropolis–Hastings correction as described in the following section.

3.2 Hamiltonian Monte Carlo kernel

Hamiltonian Monte Carlo [HMC, Neal, 1993, Duane et al., 1987] is a Metropolis–Hastings (MH) algorithm on phase space that targets $\tilde{\pi}$ with the time discretized Hamiltonian dynamics $\hat{\Phi}_{\varepsilon, L}(q_0, p_0) = (q_L, p_L)$ as a proposal. From a state $(Q_n, P_n) \in \mathbb{R}^d \times \mathbb{R}^d$, at iteration $n \geq 0$,

1. sample a velocity $P_n^* \sim \mathcal{N}(0_d, I_d)$, independently of other variables, and set $(q_0, p_0) = (Q_n, P_n^*)$;
2. perform leap-frog integration to obtain $(q_L, p_L) = \hat{\Phi}_{\varepsilon, L}(q_0, p_0)$;
3. with probability $\alpha((q_0, p_0), (q_L, p_L))$, set $(Q_{n+1}, P_{n+1}) = (q_L, -p_L)$, otherwise set $(Q_{n+1}, P_{n+1}) = (Q_n, P_n)$.

Since the leap-frog integrator preserves **P1** and **P3**, the MH acceptance probability is given by

$$\alpha((q, p), (q', p')) = \min(1, \exp(E(q, p) - E(q', p'))), \quad (8)$$

for $(q, p), (q', p') \in \mathbb{R}^d \times \mathbb{R}^d$. As this constructs a $\tilde{\pi}$ -invariant Markov chain $(Q_n, P_n)_{n \geq 0}$ on phase space, the marginal chain $(Q_n)_{n \geq 0}$ is a π -invariant Markov chain. We can write the Markov transition kernel of the marginal chain as

$$\begin{aligned} K_{\varepsilon, L}(q, A) &= \int_{\mathbb{R}^d} \mathbb{I}_A \left(\hat{\Phi}_{\varepsilon, L}^\circ(q, p) \right) \alpha \left((q, p), \hat{\Phi}_{\varepsilon, L}(q, p) \right) \mathcal{N}(p; 0_d, I_d) dp \\ &\quad + \delta_q(A) \int_{\mathbb{R}^d} \left\{ 1 - \alpha \left((q, p), \hat{\Phi}_{\varepsilon, L}(q, p) \right) \right\} \mathcal{N}(p; 0_d, I_d) dp, \end{aligned} \quad (9)$$

for $q \in \mathbb{R}^d, A \in \mathcal{B}(\mathbb{R}^d)$. Irreducibility and geometric ergodicity of $K_{\varepsilon, L}$ have recently been established rigorously in Durmus et al. [2017]; see also Cances et al. [2007], Livingstone et al. [2016] for previous works. These results can be used to verify **A1** in Section 1.2.

3.3 Coupled Hamiltonian Monte Carlo kernel

Similarly to Section 2.2, we now consider coupling two HMC chains $(Q_n^i, P_n^i)_{n \geq 0}, i = 1, 2$ using the following procedure. From two states $(Q_n^i, P_n^i), i = 1, 2$, at iteration $n \geq 0$,

1. sample a velocity $P_n^* \sim \mathcal{N}(0_d, I_d)$, independently of other variables, and for $i = 1, 2$, set $(q_0^i, p_0^i) = (Q_n^i, P_n^*)$;
2. for $i = 1, 2$, perform leap-frog integration to obtain $(q_L^i, p_L^i) = \hat{\Phi}_{\varepsilon, L}(q_0^i, p_0^i)$;
3. sample $U \sim \mathcal{U}[0, 1]$;
4. for $i = 1, 2$, if $U \leq \alpha((q_0^i, p_0^i), (q_L^i, p_L^i))$, set $(Q_{n+1}^i, P_{n+1}^i) = (q_L^i, -p_L^i)$, otherwise set $(Q_{n+1}^i, P_{n+1}^i) = (Q_n^i, P_n^i)$.

The above procedure amounts to running two HMC chains with common random numbers. We denote the associated coupled transition kernel on the position coordinates as $\bar{K}_{\varepsilon, L}((q^1, q^2), A^1 \times A^2)$ for $q^1, q^2 \in \mathbb{R}^d$ and $A^1, A^2 \in \mathcal{B}(\mathbb{R}^d)$. Marginally we have $\bar{K}_{\varepsilon, L}((q^1, q^2), A^1 \times \mathbb{R}^d) = K_{\varepsilon, L}(q^1, A^1)$ and $\bar{K}_{\varepsilon, L}((q^1, q^2), \mathbb{R}^d \times A^2) = K_{\varepsilon, L}(q^2, A^2)$. We suppose that (Q_0^1, Q_0^2) are initialized according to π_0 independently, and (P_0^1, P_0^2) with an arbitrary distribution on \mathbb{R}^{2d} . We will write $\mathbb{P}_{\varepsilon, L}$ as the law of the coupled HMC chains $(Q_n^i, P_n^i)_{n \geq 0}, i = 1, 2$ and $\mathbb{E}_{\varepsilon, L}$ to denote expectation with respect to $\mathbb{P}_{\varepsilon, L}$.

We now establish that the relaxed meeting time $\tau_\delta = \inf \{n \geq 0 : |Q_n^1 - Q_n^2| \leq \delta\}$ for any $\delta > 0$ has geometric tail. The following result can be used to establish **A2** for the algorithm that will be introduced in the next section.

Theorem 1. *Suppose that the potential U is twice continuously differentiable, the gradient of U is globally β -Lipschitz and there exists a compact set $S \in \mathcal{B}(\mathbb{R}^d)$ with $\text{Leb}_d(S) > 0$ such that the restriction of U to S denoted by $U|_S : S \rightarrow \mathbb{R}$ is α -strongly convex. Then there exists $\tilde{\varepsilon} > 0$, $\tilde{L} \in \mathbb{N}$, $C \in \mathbb{R}_+$ and $\gamma \in (0, 1)$ such that*

$$\mathbb{P}_{\varepsilon, L}(\tau_\delta > n) \leq C\gamma^n, \quad n \in \mathbb{N}, \quad (10)$$

for any $\varepsilon < \tilde{\varepsilon}$ and $L > \tilde{L}$ satisfying $\varepsilon L < \tilde{\varepsilon} \tilde{L}$.

Proof. We first establish that the coupled HMC kernel is Leb_{2d} -irreducible by adapting the arguments in Durmus et al. [2017, proof of Theorem 2] to our coupling. Under the Lipschitz assumption on ∇U , the arguments in Durmus et al. [2017, proof of Theorem 2] imply that for any $L \in \mathbb{N}$, there exists $\tilde{\varepsilon}_L > 0$ such that the mapping $p \mapsto \hat{\Phi}_{\varepsilon, L}^\circ(q, p)$ is a continuously differentiable diffeomorphism from \mathbb{R}^d to \mathbb{R}^d for $q \in \mathbb{R}^d$ and $\varepsilon < \tilde{\varepsilon}_L$. Hence the mapping

$$p \mapsto \bar{\Phi}_{\varepsilon, L}(q, q', p) := \left(\hat{\Phi}_{\varepsilon, L}^\circ(q, p), \hat{\Phi}_{\varepsilon, L}^\circ(q', p) \right)$$

from \mathbb{R}^d to \mathbb{R}^{2d} is also a continuously differentiable diffeomorphism for $(q, q') \in \mathbb{R}^{2d}$ and $\varepsilon < \tilde{\varepsilon}_L$. Writing $\bar{\Phi}_{\varepsilon, L}^{-1} : \mathbb{R}^{2d} \rightarrow \mathbb{R}^d$ as the inverse function, by a change of variables,

$$\begin{aligned} \bar{K}_{\varepsilon, L}((q^1, q^2), A) &\geq \int_{\mathbb{R}^d} \int_0^1 \mathbb{I}_A \left(\hat{\Phi}_{\varepsilon, L}^\circ(q^1, p), \hat{\Phi}_{\varepsilon, L}^\circ(q^2, p) \right) \prod_{i=1}^2 \mathbb{I} \left(u \leq \alpha \left((q^i, p), \hat{\Phi}_{\varepsilon, L}^\circ(q^i, p) \right) \right) \mathcal{N}(p; 0_d, I_d) du dp \\ &= \int_{\mathbb{R}^d} \int_0^1 \mathbb{I}_A(\bar{q}) \prod_{i=1}^2 \mathbb{I} \left(u \leq \alpha \left((q^i, \bar{\Phi}_{\varepsilon, L}^{-1}(\bar{q})), \hat{\Phi}_{\varepsilon, L}^\circ(q^i, \bar{\Phi}_{\varepsilon, L}^{-1}(\bar{q})) \right) \right) \mathcal{N} \left(\bar{\Phi}_{\varepsilon, L}^{-1}(\bar{q}); 0_d, I_d \right) \left| \det \left(J_{\bar{\Phi}_{\varepsilon, L}^{-1}}(\bar{q}) \right) \right| du d\bar{q} \\ &\geq \text{Leb}_{2d}(A) \inf_{\bar{q} \in A} \left\{ \min_{i=1, 2} \alpha \left((q^i, \bar{\Phi}_{\varepsilon, L}^{-1}(\bar{q})), \hat{\Phi}_{\varepsilon, L}^\circ(q^i, \bar{\Phi}_{\varepsilon, L}^{-1}(\bar{q})) \right) \mathcal{N} \left(\bar{\Phi}_{\varepsilon, L}^{-1}(\bar{q}); 0_d, I_d \right) \left| \det \left(J_{\bar{\Phi}_{\varepsilon, L}^{-1}}(\bar{q}) \right) \right| \right\}, \end{aligned}$$

for all $A \in \mathcal{B}(\mathbb{R}^{2d})$, where $J_{\bar{\Phi}_{\varepsilon, L}^{-1}}$ denotes the Jacobian matrix of $\bar{\Phi}_{\varepsilon, L}^{-1}$ (with the convention $0 \times +\infty = 0$). It follows that $\bar{K}_{\varepsilon, L}$ is aperiodic and irreducible with respect to the Lebesgue measure on \mathbb{R}^{2d} .

For any real-valued measurable function $f : \Omega \rightarrow \mathbb{R}$, we write its level sets as $L_f(\ell) = \{x \in \Omega : f(x) \leq \ell\}$ for $\ell \in \mathbb{R}$. Define the kinetic energy function $K(p) = |p|^2/2$, the levels $\underline{U} > \inf_{q \in S} U(q)$ and $\bar{U} < \sup_{q \in S} U(q)$ such that $\underline{U} < \bar{U}$, and the sets $C_\ell = L_{U|_S}(\ell) \times L_K(\bar{U} - \ell) \subset L_E(\bar{U})$ and $\tilde{C}_\ell = L_{U|_S}(\ell) \times L_{U|_S}(\ell) \times L_K(\bar{U} - \ell)$ for $\ell \in (\underline{U}, \bar{U})$. Since $\text{Leb}_d(L_{U|_S}(\ell)) > 0$ for $\ell \in (\underline{U}, \bar{U})$ under the assumptions on U , Leb_{2d} -irreducibility of $\bar{K}_{\varepsilon, L}$ implies for any $L \in \mathbb{N}$ and $\varepsilon < \tilde{\varepsilon}_L$, there exists $N \in \mathbb{N}$ such that

$$\mathbb{P}_{\varepsilon, L}(Q_N^1 \in L_{U|_S}(\ell), Q_N^2 \in L_{U|_S}(\ell)) > 0.$$

When both chains enter the set $L_{U|_S}(\ell)$, it follows from Lemma 1 that there exist $\tilde{T} > 0$ and $\rho_0 < 1$ such that

$$|\Phi_T^\circ(Q_N^1, P_N^*) - \Phi_T^\circ(Q_N^2, P_N^*)| \leq \rho_0 |Q_N^1 - Q_N^2|,$$

for all $(Q_N^1, Q_N^2, P_N^*) \in \tilde{C}_\ell$ and $T < \tilde{T}$. Hence we have

$$\mathbb{P}_{\varepsilon, L} (|\Phi_T^\circ(Q_N^1, P_N^*) - \Phi_T^\circ(Q_N^2, P_N^*)| \leq \rho_0 |Q_N^1 - Q_N^2| \quad | \quad Q_N^1 \in L_{U|_S}(\ell), Q_N^2 \in L_{U|_S}(\ell)) > 0.$$

By triangle inequality, consistency of the leap-frog integrator (6) and compactness of \tilde{C}_ℓ , there exists $\varepsilon_0 \leq \tilde{\varepsilon}_L$, $L_0 \in \mathbb{N}$ and $\rho_1 < 1$ such that

$$\mathbb{P}_{\varepsilon, L} \left(|\hat{\Phi}_{\varepsilon, L}^\circ(Q_N^1, P_N^*) - \hat{\Phi}_{\varepsilon, L}^\circ(Q_N^2, P_N^*)| \leq \rho_1 |Q_N^1 - Q_N^2| \quad | \quad Q_N^1 \in L_{U|_S}(\ell), Q_N^2 \in L_{U|_S}(\ell) \right) > 0,$$

for $\varepsilon < \varepsilon_0$ and $L > L_0$ satisfying $\varepsilon L = T$. Again by consistency of the leap-frog integrator (7) and compactness of C_ℓ , it follows from (8) that there exist $\varepsilon_1 \leq \varepsilon_0$, $L_1 \geq L_0$ and $\eta_0 < 1/2$ such that

$$\mathbb{P}_{\varepsilon, L} \left(Q_{N+1}^i = \hat{\Phi}_{\varepsilon, L}^\circ(Q_N^i, P_N^*) \quad | \quad (Q_N^i, P_N^*) \in C_\ell \right) \geq 1 - \eta_0,$$

for $i = 1, 2$ and $\varepsilon < \varepsilon_1$, $L > L_1$ satisfying $\varepsilon L = T$. By Fréchet's inequality, the probability of accepting both proposals satisfies

$$\mathbb{P}_{\varepsilon, L} \left(Q_{N+1}^1 = \hat{\Phi}_{\varepsilon, L}^\circ(Q_N^1, P_N^*), Q_{N+1}^2 = \hat{\Phi}_{\varepsilon, L}^\circ(Q_N^2, P_N^*) \quad | \quad (Q_N^1, Q_N^2, P_N^*) \in \tilde{C}_\ell \right) > 0,$$

therefore

$$\mathbb{P}_{\varepsilon, L} (|Q_{N+1}^1 - Q_{N+1}^2| \leq \rho_1 |Q_N^1 - Q_N^2| \quad | \quad Q_N^1 \in L_{U|_S}(\ell), Q_N^2 \in L_{U|_S}(\ell)) > 0.$$

To iterate this argument, note first that if $(q, p) \in C_\ell$ then continuity of U and the mapping $t \mapsto \Phi_t^\circ(q, p)$ implies $\Phi_t^\circ(q, p) \in L_{U|_S}(\bar{U})$ for any $t \in \mathbb{R}_+$. Owing to time discretization, we only have $\hat{\Phi}_t^\circ(q, p) \in L_{U|_S}(\bar{U} + \eta_1)$ for $(q, p) \in C_\ell$ and some $\eta_1 > 0$, by another application of (7). It follows that there exists a number of iterations $I \in \mathbb{N}$ that depends on ρ_1 , and an initial level $\ell_0 \in (\underline{U}, \bar{U})$ depending on I and η_1 such that

$$\mathbb{P}_{\varepsilon, L} (|Q_{N+I}^1 - Q_{N+I}^2| \leq \delta \quad | \quad Q_N^1 \in L_{U|_S}(\ell_0), Q_N^2 \in L_{U|_S}(\ell_0)) > 0.$$

Therefore we can conclude (10) by applying Williams [1991, Exercise E.10.5]. \square

Under similar conditions, Durmus et al. [2017] provide a convergence result for the marginal HMC chains, which can be used to check **A1**; see also Cances et al. [2007], Livingstone et al. [2016], Mangoubi and Smith [2017] and Tweedie [1983] for the finiteness of moments.

It is worth noting that the distance between chains might exceed δ at some future iterations $n > \tau_\delta$, and that the event $\{|Q_n^1 - Q_n^2| \leq \delta\}$ is not an exact meeting event; thus Theorem 1 does not establish **A2**. In the next section, we combine coupled HMC kernels with another kernel designed to prompt exact meetings, which would occur with large probability when the two chains are close.

4 Unbiased Hamiltonian Monte Carlo estimators

The construction of Jacob et al. [2017b] requires two chains that meet exactly. One possibility here is the approach of Glynn and Rhee [2014], which involves the introduction of a truncation variable. Instead we propose to use coupled Metropolis–Hastings steps to trigger exact meetings. These coupled MH steps are described in Section 4.1, and a summary of the proposed methodology combining the two coupled kernels is in Section 4.2. Section 4.3 briefly describes a further variance reduction technique.

4.1 Coupled Metropolis–Hastings steps

As in Section 1, let us denote the two chains by $(X_n)_{n \geq 0}$ and $(Y_n)_{n \geq 0}$; these correspond to the position coordinates in Section 3, propagated with a time shift, e.g. $(X_{n+1}, Y_n) \sim \hat{K}_{\varepsilon, L}((X_n, Y_{n-1}), \cdot)$. According to Theorem 1, coupled HMC chains are close to one another after some iterations. Denote the distance between the chains at step n by $\delta_n = |X_n - Y_{n-1}|$.

In a coupled MH step with Normal random walk, a pair of proposals (X^*, Y^*) is sampled from the maximal coupling of $\mathcal{N}(X_n, \Sigma)$ and $\mathcal{N}(Y_{n-1}, \Sigma)$ [Jacob et al., 2017b]. Let us consider the case where $\Sigma = \sigma^2 I_d$ for some $\sigma > 0$.

Algorithm 1 Unbiased HMC estimator $\bar{H}_{k:m}(X, Y)$ of $\pi(h)$, with tuning parameters $\omega, \sigma, \varepsilon, L, k, m$.

The kernel \bar{P}_σ refers to a coupled random walk MH kernel with proposal standard deviation σ , and maximally coupled proposals. The kernel $\bar{K}_{\varepsilon,L}$ refers to a coupled HMC kernel with step size ε , L leap-frog steps, and common initial velocity at each step. The marginal kernels are denoted by P_σ and $K_{\varepsilon,L}$ respectively.

1. Draw X_0 and Y_0 from an initial distribution π_0 , and
 - (a) with probability ω , sample $X_1 \sim P_\sigma(X_0, \cdot)$;
 - (b) otherwise sample $X_1 \sim K_{\varepsilon,L}(X_0, \cdot)$;
 - (c) set $n = 1$.
2. While $X_n \neq Y_{n-1}$ and $n < m$,
 - (a) with probability ω , sample $(X_{n+1}, Y_n) \sim \bar{P}_\sigma((X_n, Y_{n-1}), \cdot)$;
 - (b) otherwise, sample $(X_{n+1}, Y_n) \sim \bar{K}_{\varepsilon,L}((X_n, Y_{n-1}), \cdot)$;
 - (c) if $X_{n+1} = Y_n$ set $\tau = n + 1$;
 - (d) increment $n \leftarrow n + 1$.
3. Compute $H_\ell(X, Y) = h(X_\ell) + \sum_{n=\ell}^{\max(m, \tau-1)} \{h(X_{n+1}) - h(Y_n)\}$ for $\ell \in [k : m]$,
and $\bar{H}_{k:m}(X, Y) = (m - k + 1)^{-1} \sum_{\ell=k}^m H_\ell(X, Y)$; or compute $\bar{H}_{k:m}(X, Y)$ as in (2).

Under the maximal coupling, we have $\mathbb{P}(X^* = Y^*) = 1 - d_{\text{TV}}(\mathcal{N}(X_n, \sigma^2 I_d), \mathcal{N}(Y_{n-1}, \sigma^2 I_d))$. The total variation can be approximated as in [Pollard \[2005\]](#). First, we have $d_{\text{TV}}(\mathcal{N}(X_n, \sigma^2 I_d), \mathcal{N}(Y_{n-1}, \sigma^2 I_d)) = \mathbb{P}(2\sigma |Z| \leq \delta_n)$, where Z is a univariate standard Normal variable and δ_n is considered fixed. Approximations of the folded Normal cumulative distribution function then lead to

$$\mathbb{P}(X^* = Y^*) = 1 - \mathbb{P}(2\sigma |Z| \leq \delta_n) = 1 - \frac{1}{\sqrt{2\pi}} \frac{\delta_n}{\sigma} + \mathcal{O}\left(\frac{\delta_n^2}{\sigma^2}\right), \quad \text{as } \frac{\delta_n}{\sigma} \rightarrow 0.$$

To achieve $\mathbb{P}(X^* = Y^*) = s$ for some desired probability s , we can choose σ as approximately $\delta_n / (\sqrt{2\pi} (1 - s))$. The proposed values (X^*, Y^*) are then accepted as the next states according to MH acceptance ratios, i.e. if $U \leq \min(1, \pi(X^*)/\pi(X_n))$ and $U \leq \min(1, \pi(Y^*)/\pi(Y_{n-1}))$ respectively, where a single uniform variable $U \sim \mathcal{U}[0, 1]$ is used for both chains.

If σ is small compared to the spread of the target density function, the probability of jointly accepting the proposals is high. On the other hand, σ needs to be large compared to $\delta_n = |X_n - Y_{n-1}|$ for the event $\{X^* = Y^*\}$ to frequently occur. This leads to a trade-off; in numerical experiments, for pairs of chains propagated using the coupled HMC kernel $\bar{K}_{\varepsilon,L}$, we can monitor both the distance δ_n and the target density values to guide the choice of σ . We will choose a fixed value of σ for all coupled MH steps, and leave adaptive strategies, where σ would be e.g. chosen according to δ_n , for future research. Hereafter we denote by P_σ and \bar{P}_σ the marginal and coupled kernels associated with the MH steps.

4.2 Combining kernels

We propose to use both coupled HMC and MH kernels through a mixture. The coupled HMC kernel is expected to bring the two chains close to one another, while the coupled MH kernel enables exact meetings when the chains are already close. In a mixture of kernels, at each step, the MH kernel is chosen with probability ω , otherwise the HMC kernel is chosen. The procedure is described in Algorithm 1. Note that **A3** is satisfied by design for coupled chains generated by this algorithm. As the resulting coupled mixture kernel inherits properties of the coupled MH kernel, **A2** can in principle be verified by simply relying on the properties of coupled MH kernels established in [Jacob et al. \[2017b\]](#). However, we stress here that Theorem 1 provides some insight on the role of coupled HMC steps on the efficiency of the proposed estimator.

We now comment on the computational cost of Algorithm 1. Assume for simplicity that the cost of evaluating the target density is approximately equal to that of evaluating its gradient. Each HMC step is then $L + 1$ times more expensive than a MH step. If we choose a small value for ω , such as 0.1 or 0.05, the cost of the MH steps becomes negligible. Secondly, the cost of running two chains is approximately twice the cost of running each chain

until meeting occurs. Thereafter, only one chain needs to be propagated up to step m . If we choose m to be much larger than τ with high probability, the cost of Algorithm 1 is therefore comparable to the cost of m HMC iterations.

The efficiency of the unbiased HMC estimator depends on the mixing properties of the underlying HMC kernel, and on the contraction achieved by the coupling. Importantly, the tuning parameters ε and L that would be optimal for the marginal HMC kernel are not necessarily adequate for the coupled kernel, as illustrated in Section 5. The other tuning parameters include σ for the coupled MH step discussed above, and Jacob et al. [2017b] give recommendations for k and m : namely k can be chosen as a large quantile of the meeting times, and m such that $(m - k)/m \approx 1$, for instance $m = 10k$.

Finally, in Section 5.2 we will encounter a situation where the coupled HMC kernel contracts so quickly that the distance $|X_n - Y_{n-1}|$ becomes smaller than machine precision after a small number of iterations. The two chains can then be considered exactly identical, for all practical purposes, and the coupled MH steps become unnecessary.

4.3 Choice of weights and variance reduction

As suggested in Jacob et al. [2017a,b], the estimators $H_\ell(X, Y)$ for $\ell \in [k : m]$ given in (1), can be averaged with any weights $(w_\ell)_{\ell=k}^m$ such that $\sum_{\ell=k}^m w_\ell = 1$. The estimator $\bar{H}_{k:m}(X, Y)$ in (2) corresponds to weights equal to $(m - k + 1)^{-1}$. For an arbitrary choice $(w_\ell)_{\ell=k}^m$, the estimator $\sum_{\ell=k}^m w_\ell H_\ell(X, Y)$ is unbiased and its variance is given by $w^T \Sigma_H w$, where Σ_H denotes the $(m - k + 1) \times (m - k + 1)$ covariance matrix of the estimators (H_k, \dots, H_m) . To minimize such a variance without violating the sum constraint, we solve the system

$$\begin{pmatrix} & & 1 \\ \Sigma_H & & \vdots \\ & & 1 \\ 1 & \dots & 1 & 0 \end{pmatrix} \begin{pmatrix} w_k \\ \vdots \\ w_m \\ \lambda \end{pmatrix} = \begin{pmatrix} 0 \\ \vdots \\ 0 \\ 1 \end{pmatrix},$$

where λ is a Lagrange multiplier, for a computational cost of order $(m - k + 1)^3$. The matrix Σ_H can be approximated from i.i.d. realizations of H_ℓ for $\ell \in [k : m]$. The resulting weights can then be used to reduce the variance of $\bar{H}_{k:m}(X, Y)$, especially if the original MCMC chain exhibits strong autocorrelations.

5 Numerical illustrations

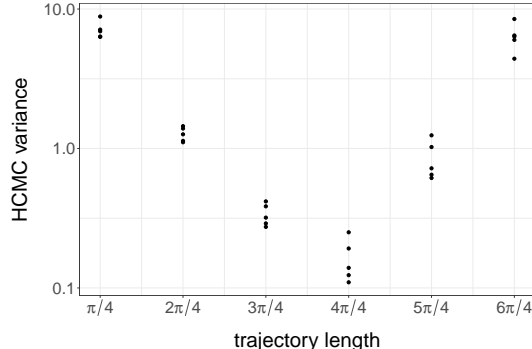
We investigate some key aspects of the proposed unbiased HMC estimator, such as its efficiency compared to standard HMC estimators. As in the rest of the article, we choose a Normal distribution for the initial velocities at each HMC step, and a unit mass matrix; other choices are possible [Girolami and Calderhead, 2011, Livingstone et al., 2017].

In all experiments, whenever the test function h is not specified, it is chosen as $h : x \mapsto x_1$, so that $\pi(h)$ is simply the mean of the first target marginal distribution. The asymptotic variance of an MCMC estimator refers to the variance appearing in the central limit theorem satisfied by $N^{-1} \sum_{n=0}^N h(X_n)$ as $N \rightarrow \infty$, where $(X_n)_{n \geq 0}$ is the chain generated by the algorithm. Here, these asymptotic variances are approximated with the `spectrum0` function of the `coda` package [Plummer et al., 2006]. For unbiased estimators, we define the asymptotic efficiency as variance multiplied by expected cost [Glynn and Whitt, 1992]. This accounts for the fact that, in a given computing budget, more estimators can be averaged over if each one can be produced faster. For the estimator $\bar{H}_{k:m}(X, Y)$ in (2), the expected computing time $\mathbb{E}[\max(\tau, m)]$ and the variance $\mathbb{V}[\bar{H}_{k:m}(X, Y)]$ are approximated by empirical averages of independent realizations.

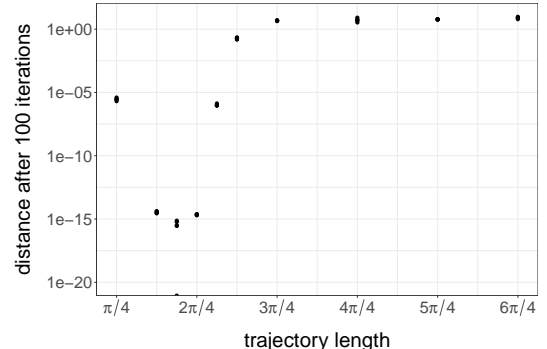
5.1 Multivariate Normal distribution

Let the target π be a multivariate Normal $\mathcal{N}(0_d, \Sigma_\pi)$ with $d = 250$ and with the (i, j) -entry of Σ_π equal to $\exp(-|i - j|)$. In this example we discuss the choice of trajectory length, defined as the product εL , and the use of coupled MH kernels to trigger exact meetings.

We fix the number of leap-frog steps to $L = 20$ and vary the step size ε so that the trajectory length εL spans between 0 and $3\pi/2$, where π here denotes the mathematical constant. The initial distribution π_0 is chosen as the target. For each trajectory length, the asymptotic variance of HMC computed from 5,000 iterations is shown in Figure 1a. The optimal trajectory length is close to the value π , which is consistent with the analytical solution in Section 2.2. For such a trajectory length, the asymptotic variance is smaller than the variance obtained with perfect samples from the target, thanks to negative auto-correlations.

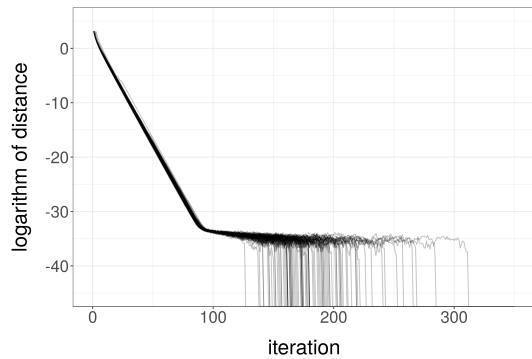


(a) HMC asymptotic variance against trajectory length εL .

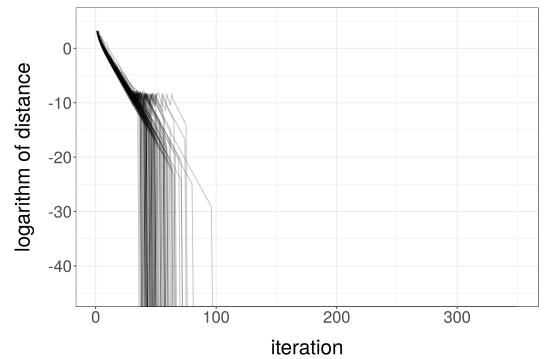


(b) Distance after 100 coupled HMC iterations against trajectory length εL .

Figure 1: In the multivariate Normal example of Section 5.1, asymptotic variance for the estimation of $\int x_1 \pi(dx)$ using HMC, computed using chains of length 5,000 started at stationarity (left). Euclidean distance between the 100-th iterate of coupled HMC chains (right). The number of leap-frog steps is set to $L = 20$, which implicitly determines the step size ε for each trajectory length εL . Each dot corresponds to one of 5 independent runs.



(a) Log-distance between coupled HMC chains against iterations.



(b) Log-distance between coupled chains propagated with a mixture of HMC and MH kernels, against iterations.

Figure 2: In the multivariate Normal example of Section 5.1, distance between coupled HMC chains against number of iterations (left), and between chains propagated with the the mixture of HMC and MH kernels, with $\sigma = 10^{-5}$ and $\omega = 0.1$ (right). Each line corresponds to one of 100 independent runs.

We then run 100 iterations of coupled HMC and compute the Euclidean distance between the two final states. The resulting distances are shown in Figure 1b. Lengths around the value $\pi/2$ lead to the smallest distances, consistently with the analytical reasoning of Section 2.2. Moreover, there is a range of lengths that lead to contraction. On the other hand, the optimal length for the HMC estimator, which was the value π , does not lead to visible contraction after 100 iterations. Therefore, the proposed coupling contracts most with tuning parameters that are not optimal for the underlying HMC algorithm, which results in a loss of efficiency.

Based on Figure 1b, we set $\varepsilon L = \pi/2$, $L = 20$ and run coupled chains, 100 times independently, until their distances is less than machine precision. In Figure 2a these distances are plotted on a logarithmic scale against iterations; the lines drop when the distances fall below machine precision, which occurs between iterations 127 and 312. The distances are already very small after a few dozen iterations. We implement the proposed algorithm with a mixture of kernels described in Section 4.2, with $\sigma = 10^{-5}$ and $\omega = 0.1$, and plot the resulting distances in Figure 2b. All meeting times then occur between iterations 36 and 97. The MH steps thus successfully manage to trigger exact meetings.

We set $k = 50$ and $m = 500$ to produce $R = 100$ unbiased estimators of $\int x_1 \pi(dx)$ as in (2). The asymptotic efficiency is approximately equal to 1.96. The asymptotic variance of HMC obtained with $\varepsilon L = \pi$ was found to be approximately 0.16, averaging the 5 runs shown in Figure 1a. Therefore, the proposed estimator is about 12 times less efficient than the original HMC algorithm when optimally tuned. Depending on hardware, this can be

considered an acceptable loss in exchange for complete parallelism, among other advantages of unbiased estimators argued e.g. in [Rhee \[2013\]](#), [Jacob et al. \[2017b\]](#). Unbiased estimators could also be obtained from variants of HMC where the number of leap-frog steps L is random, and possibly adaptive, which might reduce the efficiency loss.

5.2 Truncated Normal distribution

We consider Hamiltonian Monte Carlo on truncated Normal distributions, with truncations defined by linear and quadratic inequalities. In this setting [Pakman and Paninski \[2014\]](#) show that Hamiltonian dynamics can be solved, resulting in trajectories that bounce off the constraints. An R package implementing the method of [Pakman and Paninski \[2014\]](#) is available online [[Pakman, 2012](#)]. Using this package, the implementation of the proposed method only involved simple modifications.

We consider two of the examples in [Pakman and Paninski \[2014\]](#), where a bivariate Normal distribution is truncated by two linear and two quadratic constraints respectively. A thousand HMC samples are shown in Figure 3 (top row). The first distribution is a bivariate Normal, with unit covariance matrix and mean $(4, 4)$, restricted to the set $\{x_1 \leq x_2 \leq 1.1x_1\} \subset \mathbb{R}^2$ (Figure 3a). The second distribution is a bivariate standard Normal restricted to the set $\{(x_1 - 4)^2/32 + (x_2 - 1)^2/8 \leq 1\} \cap \{4x_1^2 + 8x_2^2 - 2x_1x_2 + 5x_2 \geq 1\} \subset \mathbb{R}^2$ (Figure 3b). We use the value $\pi/2$ as a trajectory length, as advocated in [Pakman and Paninski \[2014\]](#). As for the initial distribution π_0 , we use a point mass at $(2, 2.1)$ for the first target, and at $(2, 0)$ for the second one.

In this example, the proposed coupling induces a contraction that leads to distances between trajectories becoming smaller than machine precision, after a few iterations. Therefore, we do not need to resort to coupled MH steps: we can define the meeting times directly as the first times for which distances are less than machine precision. Histograms of such meeting times are shown in Figure 3 for both targets (bottom row). They indicate that small values of k and m could be chosen, effectively leading to the possibility of running very short HMC chains in parallel in a principled way.

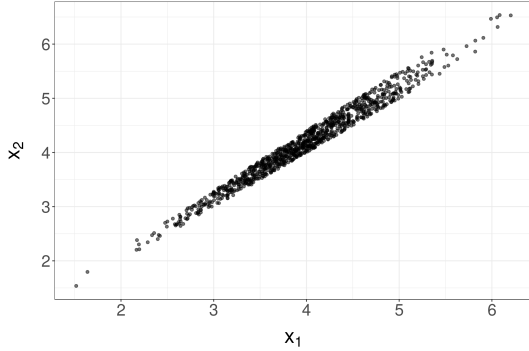
5.3 Logistic regression

We consider a Bayesian logistic regression as in [Hoffman and Gelman \[2014\]](#), on the classic German credit data set. Including pairwise interactions, the covariates are in a matrix X with $N = 1000$ rows and $p = 300$ columns, which we standardize by column. The parameters are the intercept $\alpha \in \mathbb{R}$, coefficients $\beta \in \mathbb{R}^p$, and a prior variance $\sigma^2 \in \mathbb{R}_+$ on intercept and coefficients. The likelihood specifies that the binary outcome Y_i satisfies $\mathbb{P}(Y_i = 1|X_i, \alpha, \beta) = (1 + \exp(-\alpha - X_i^T \beta))^{-1}$ for all $i \in [1 : N]$. The prior specifies $\alpha|\sigma^2 \sim \mathcal{N}(0, \sigma^2)$ and $\beta_j|\sigma^2 \sim \mathcal{N}(0, \sigma^2)$, for all $j \in [1 : p]$, and an Exponential distribution with rate $\lambda = 0.01$ for σ^2 . We transform σ^2 into $\log \sigma^2$, so that each parameter lies in \mathbb{R} . The target π is the posterior distribution of $(\alpha, \beta, \log \sigma^2)$, of dimension $d = p + 2 = 302$. We use an independent standard Normal for each parameter to initialize the chains, which defines π_0 .

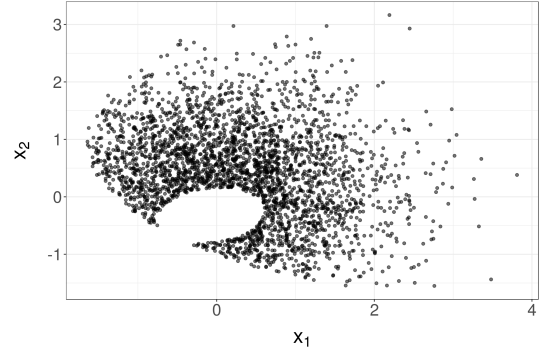
We set $L = 20$ and vary ε so that the trajectory length εL is in the range $[0.1, 0.5]$. For each length, we run 10,000 HMC iterations, discard the first 5,000 as burn-in, and use the remaining 5,000 samples to approximate the asymptotic variance of HMC for the estimation of $\int x_1 \pi(dx)$, which here is the posterior expectation of the intercept. The results of independent runs are shown in Figure 4a. Coupled HMC chains are then run for 1,000 iterations, and the distances between the final states are shown in Figure 4b. Again, the optimal choice of εL for the asymptotic variance of HMC is not optimal in terms of contraction. However, contrarily to the example of Section 5.1, here each of the considered trajectory lengths yields some contraction.

Using the length $\varepsilon L = 0.1$, we then proceed with Algorithm 1 of Section 4.2, using $\sigma = 10^{-5}$ and $\omega = 0.05$. Over 100 independent experiments, we compute the distance between the coupled chains, using two different initializations. The first is the standard Normal distribution on each parameter as above, leading to the distances plotted in Figure 5a. The observed meeting times occur between iterations 256 and 535. Using $k = 100$ and $m = 1,000$, we produce 100 independent estimators $\bar{H}_{k:m}(X, Y)$ from these coupled chains, in order to approximate the marginal means and variances of the target. With these values, we construct a Normal approximation of the target, with a diagonal covariance matrix, and use this Normal as a new initial distribution π_0 . For this better initialization, the distance traces are shown in Figure 5b. The observed meeting times occur between iterations 192 and 422, and the plot shows that the distances decrease faster than with the previous initialization. The vertical upward jumps in Figure 5 correspond to events where one chain accepts its HMC proposal while the other chain does not.

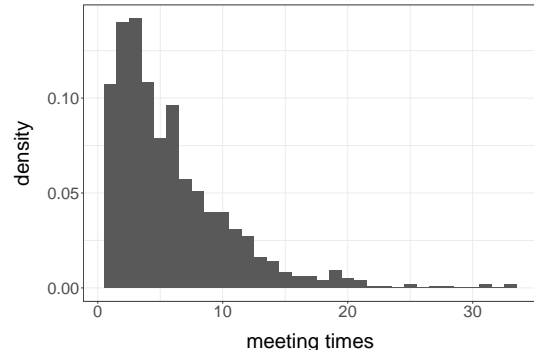
With this better initialization, again using $k = 100$ and $m = 1,000$, we produce $R = 1,000$ independent estimators of $\int x_1 \pi(dx)$. The asymptotic efficiency is found to be approximately 0.40. The asymptotic variance of HMC obtained with $\varepsilon L = 0.3$ was found to be approximately 0.09, and with $\varepsilon L = 0.1$ approximately 0.33;



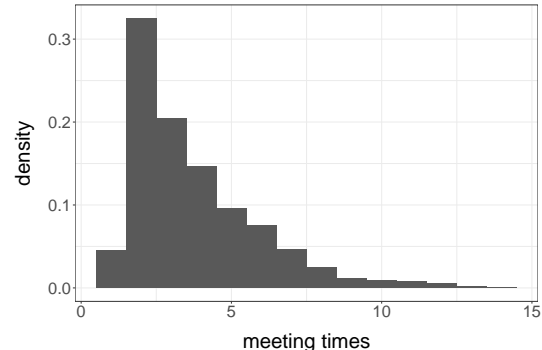
(a) HMC samples approximating a bivariate Normal truncated by two linear constraints.



(b) HMC samples approximating a bivariate Normal truncated by two quadratic constraints.

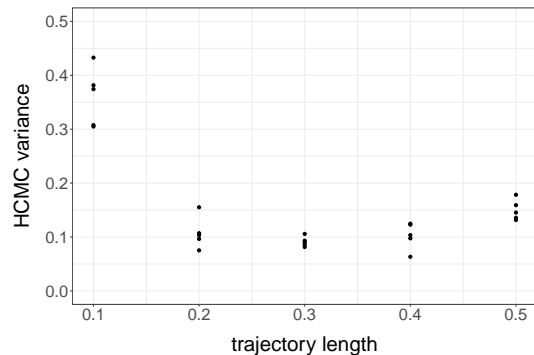


(c) Meeting times for the bivariate Normal with linear constraints.

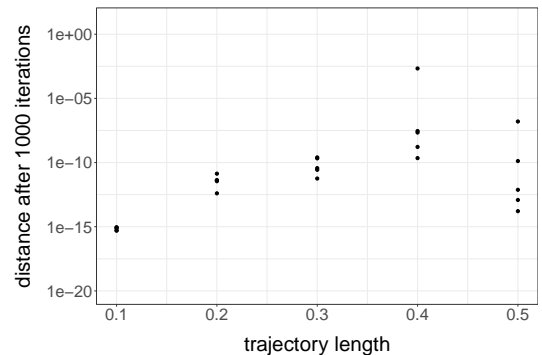


(d) Meeting times for the bivariate Normal with quadratic constraints.

Figure 3: In the truncated Normal example of Section 5.2, scatter plot of 1,000 HMC samples for a bivariate Normal truncated by two linear constraints (top left), and two quadratic constraints (top right). Histogram of 1,000 meeting times, defined as first times for which the distance is smaller than machine precision, for coupled HMC chains targeting the bivariate Normal with linear constraints (bottom left), and with quadratic constraints (bottom right).



(a) HMC asymptotic variance against trajectory length εL .



(b) Distance after 1,000 coupled HMC steps against trajectory length εL .

Figure 4: In the logistic regression example of Section 5.3, asymptotic variance for the estimation of $\int x_1 \pi(dx)$ using HMC, computed using chains of length 10,000 started from an independent standard Normal distribution for each parameter, and discarding a burn-in of 5,000 steps (left). Euclidean distance between the 1,000-th iterate of coupled HMC chains (right). The number of leap-frog steps is set to $L = 20$, which implicitly determines the step size ε for each trajectory length εL . Each dot corresponds to one of 5 independent runs.

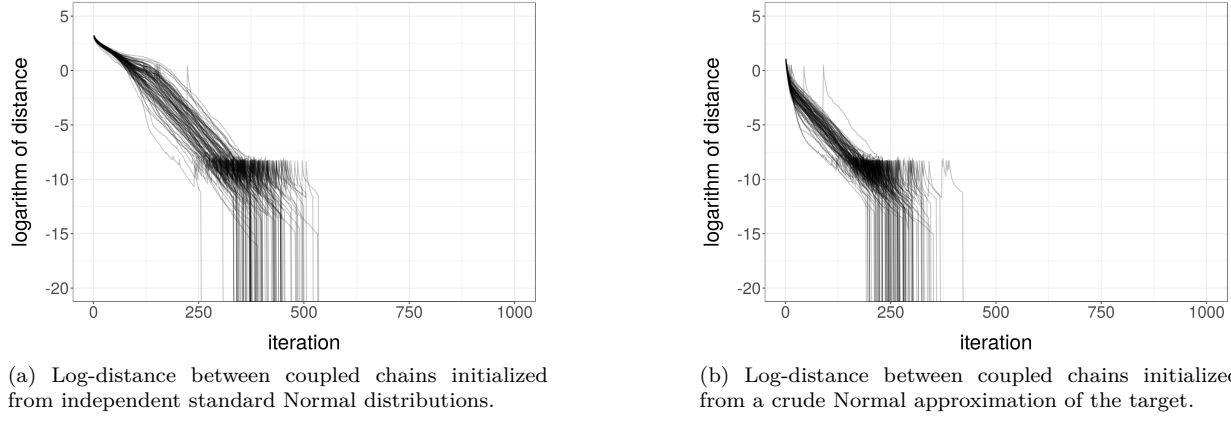


Figure 5: In the logistic regression example of Section 5.3, distance between coupled chains initialized from independent standard Normal distributions for each parameter against number of iterations (left), and initialized from a Normal approximation of the target (right). The Normal approximation is obtained by estimating the 302 marginal means and variances of the target distribution. In both cases the chains are propagated using a mixture of HMC and MH kernels, with $\sigma = 10^{-5}$ and $\omega = 0.05$, and the HMC kernel uses $L = 20$ and $\varepsilon L = 0.1$. Each line corresponds to one of 100 independent runs.

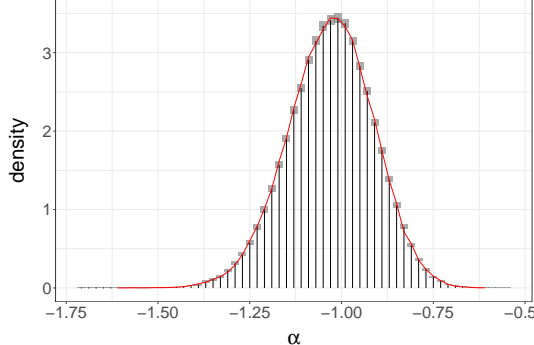
these were obtained from 10^5 HMC iterations after discarding 5,000 iterations as burn-in. Therefore, the proposed estimator is about 4 times less efficient than the original HMC estimator when optimally tuned, or more precisely, for the optimal value of ε given a fixed value $L = 20$. We could also use $\varepsilon L = 0.3$ for the unbiased HMC estimator, according to Figure 4b, but the meeting times would then be longer, and the potential for parallelization would thus be reduced.

From the coupled chains, histograms can be produced by binning a dimension of the space and estimating posterior masses of these bins, which are integrals of indicator functions [Jacob et al., 2017b]. Histograms of α and β_1 under the posterior distribution are shown in Figure 6. The vertical bars indicate the point estimates of posterior masses, and gray rectangles represent 95% confidence intervals based on the central limit theorem. The overlaid red curves show kernel density estimates obtained from 10^5 HMC samples, after discarding a burn-in of 5,000 steps, and using $L = 20$ and $\varepsilon L = 0.3$. Taking these kernel density estimates as ground truth, the narrowness of confidence intervals reflects the accuracy of the proposed estimators. We stress that these confidence intervals are based on the central limit theorem for averages of independent variables, and are therefore justified in the limit of number of independent estimators, all of which can be computed in parallel.

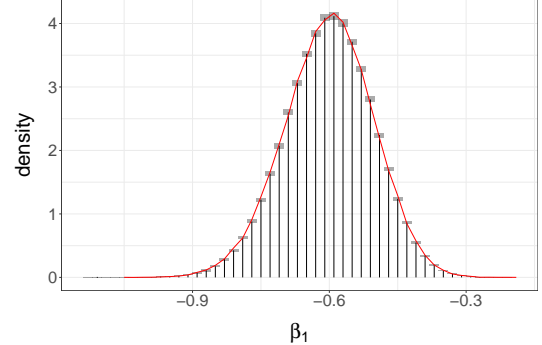
6 Discussion

Coupled Hamiltonian Monte Carlo chains can be combined to generate unbiased estimators of integrals with respect to target distributions. With adequate couplings, such chains become exactly equal after a random number of steps. The proposed approach involves a simple coupling of Hamiltonian Monte Carlo kernels, based on common random numbers, that generates chains converging to one another. Combined with coupled random walk Metropolis–Hastings steps, the approach leads to estimators that can be produced independently in parallel and averaged. The method is demonstrated on three examples, and a contraction property of coupled HMC kernels is formally established under strong log-concavity of the target on parts of the state space. Recently, Mangoubi and Smith [2017] have proposed a much deeper study of the same coupling, and have adroitly exploited it to obtain novel quantitative bounds on mixing properties of HMC. The same coupling was already discussed in Neal [2002], for the purpose of removing the burn-in bias. The exploration of further links between our proposed estimators and the circular coupling of Neal [2002] is an exciting avenue of research. The proposed couplings also enable other unbiased estimators, such as those of Glynn and Rhee [2014] which do not require exact meetings.

As seen in numerical experiments, optimal trajectory lengths for standard HMC estimators are not optimal in the coupled construction. This leads to a loss of efficiency of the proposed estimators compared to standard HMC estimators. Whether this loss is acceptable or not will likely depend on the target distribution and the available hardware. Other considerations include the construction of confidence intervals, which is arguably simpler with i.i.d. variables than with Markov chains, and the unbiased property itself, which could be appealing in various



(a) Estimated posterior of the intercept α .



(b) Estimated posterior of the coefficient β_1 .

Figure 6: In the logistic regression example of Section 5.3, histograms of the posterior distributions of the intercept α (left) and of the first coefficient β_1 (right). Vertical bars indicate point estimates of posterior mass in each bin, obtained with 1,000 unbiased HMC estimators, and 95% confidence intervals are represented by gray rectangles. Red curves represent kernel density estimates computed from 10^5 HMC iterations, considered as the ground truth.

contexts.

To improve asymptotic efficiencies, random numbers of leap-frog steps, and adaptive selection of that number based on the distance between the chains, would be interesting topics of research. A related question would be the construction of unbiased estimators from the No-U-Turn sampler of Hoffman and Gelman [2014]. Finally, the optimal weights described in Section 4.3 could potentially bring significant variance reduction in situations where HMC chains exhibit significant autocorrelations.

Acknowledgement

Pierre E. Jacob gratefully acknowledges support by the National Science Foundation through grant DMS-1712872.

References

Beskos A., Pillai N., Roberts G., Sanz-Serna J.-M., and Stuart A. The acceptance probability of the Hybrid Monte Carlo method in high-dimensional problems. In *AIP Conference Proceedings*, volume 1281, pages 23–26. AIP, 2010. [1](#)

Beskos A., Pillai N., Roberts G., Sanz-Serna J.-M., and Stuart A., 2013. Optimal tuning of the Hybrid Monte Carlo algorithm. *Bernoulli*, 19(5A):1501–1534. [1](#)

Brooks S. P., Gelman A., Jones G., and Meng X.-L., 2011. *Handbook of Markov chain Monte Carlo*. CRC press. [1](#)

Cances E., Legoll F., and Stoltz G., 2007. Theoretical and numerical comparison of some sampling methods for molecular dynamics. *ESAIM: Mathematical Modelling and Numerical Analysis*, 41(2):351–389. [5](#), [7](#)

Carpenter B., Gelman A., Hoffman M. D., Lee D., Goodrich B., Betancourt M., Brubaker M. A., Guo J., Li P., and Riddell A., 2016. Stan: a probabilistic programming language. *Journal of Statistical Software*, 20:1–37. [1](#)

Casella G., Lavine M., and Robert C. P., 2001. Explaining the perfect sampler. *The American Statistician*, 55(4):299–305. [1](#)

Duane S., Kennedy A. D., Pendleton B. J., and Roweth D., 1987. Hybrid Monte Carlo. *Physics Letters B*, 195(2):216–222. [1](#), [5](#)

Durmus A., Moulines E., and Saksman E., 2017. On the convergence of Hamiltonian Monte Carlo. *arXiv preprint arXiv:1705.00166*. [5](#), [6](#), [7](#)

Girolami M. and Calderhead B., 2011. Riemann manifold Langevin and Hamiltonian Monte Carlo methods. *Journal of the Royal Statistical Society: Series B (Statistical Methodology)*, 73(2):123–214. [9](#)

Glynn P. W. Exact simulation versus exact estimation. In *Winter Simulation Conference (WSC), 2016*, pages 193–205. IEEE, 2016. [1](#)

Glynn P. W. and Rhee C.-H., 2014. Exact estimation for Markov chain equilibrium expectations. *Journal of Applied Probability*, 51(A):377–389. [1](#), [7](#), [13](#)

Glynn P. W. and Whitt W., 1992. The asymptotic efficiency of simulation estimators. *Operations Research*, 40(3):505–520. [9](#)

Hairer E., Wanner G., and Lubich C., 2005. *Geometric numerical integration: structure-preserving algorithms for ordinary differential equations*. Springer-Verlag, New York. 5

Hoffman M. D. and Gelman A., 2014. The No-U-turn sampler: adaptively setting path lengths in Hamiltonian Monte Carlo. *Journal of Machine Learning Research*, 15(1):1593–1623. 1, 11, 14

Huber M., 2016. *Perfect simulation*, volume 148. CRC Press. 1

Jacob P. E. and Thiery A. H., 2015. On non-negative unbiased estimators. *The Annals of Statistics*, 43(2):769–784. 1

Jacob P. E., Lindsten F., and Schön T. B., 2017a. Smoothing with couplings of conditional particle filters. *arXiv preprint arXiv:1701.02002*. 1, 9

Jacob P. E., O’Leary J., and Atchadé Y. F., 2017b. Unbiased Markov chain Monte Carlo with couplings. *arXiv preprint arXiv:1708.03625*. 1, 2, 7, 8, 9, 11, 13

Leimkuhler B. and Matthews C., 2015. *Molecular Dynamics*. Springer-Verlag, New York. 5

Lelièvre T., Rousset M., and Stoltz G., 2010. *Free Energy Computations: A Mathematical Perspective*. Imperial College Press. ISBN 978-1-84816-248-8. 1, 3

Livingstone S., Betancourt M., Byrne S., and Girolami M., 2016. On the geometric ergodicity of Hamiltonian Monte Carlo. *arXiv preprint arXiv:1601.08057*. 5, 7

Livingstone S., Faulkner M. F., and Roberts G. O., 2017. Kinetic energy choice in Hamiltonian/hybrid Monte Carlo. *arXiv preprint arXiv:1706.02649*. 9

Mangoubi O. and Smith A., 2017. Rapid mixing of Hamiltonian Monte Carlo on strongly log-concave distributions. *arXiv preprint arXiv:1708.07114*. 7, 13

Mykland P., Tierney L., and Yu B., 1995. Regeneration in Markov chain samplers. *Journal of the American Statistical Association*, 90(429):233–241. 1

Neal R. M., 1993. Bayesian learning via stochastic dynamics. *Advances in neural information processing systems*, pages 475–475. 1, 5

Neal R. M. Circularly-coupled Markov chain sampling. Technical report, 9910 (revised), Department of Statistics, University of Toronto, 2002. 1, 13

Neal R. M., 2011. MCMC using Hamiltonian dynamics. *Handbook of Markov chain Monte Carlo*, 2(11). 3

Pakman A., 2012. tmg: truncated multivariate Gaussian sampling. *CRAN*. URL <https://cran.r-project.org/package=tmg>. 11

Pakman A. and Paninski L., 2014. Exact Hamiltonian Monte Carlo for truncated multivariate Gaussians. *Journal of Computational and Graphical Statistics*, 23(2):518–542. 11

Plummer M., Best N., Cowles K., and Vines K., 2006. CODA: Convergence diagnosis and output analysis for MCMC. *R News*, 6(1):7–11. URL <https://journal.r-project.org/archive/>. 9

Pollard D., 2005. *Chapter 3: Total variation distance between measures*. Asymptopia. URL <http://www.stat.yale.edu/~pollard/Courses/607.spring05/handouts/Totalvar.pdf>. 8

Rhee C.-H. *Unbiased estimation with biased samplers*. PhD thesis, Stanford University, 2013. URL <http://purl.stanford.edu/nf154yt1415>. 11

Rosenthal J. S., 1997. Faithful couplings of Markov chains: now equals forever. *Advances in Applied Mathematics*, 18(3):372 – 381. ISSN 0196-8858. 2

Rosenthal J. S., 2000. Parallel computing and Monte Carlo algorithms. *Far east journal of theoretical statistics*, 4 (2):207–236. 1

Thorisson H., 2000. *Coupling, stationarity, and regeneration*, volume 14. Springer New York. 1

Tweedie R., 1983. The existence of moments for stationary Markov chains. *Journal of Applied Probability*, 20(1): 191–196. 7

Vihola M., 2015. Unbiased estimators and multilevel Monte Carlo. *arXiv preprint arXiv:1512.01022*. 1

Williams D., 1991. *Probability with martingales*. Cambridge university press. 7